NSIDC Special Report 7
Impact of Various Processing Options on SSM/I-derived Brightness Temperatures

Julienne Stroeve
15 September 1998

National Snow and Ice Data Center
Cooperative Institute for Research in Environmental Sciences
University of Colorado, Boulder, Colorado, USA

Abstract

The processing options for the SSM/I data that NSIDC receives from Remote Sensing Systems, Inc. (RSS) have evolved over time. These include options for along-track scan corrections and sensor-to-sensor "calibrations". This document summarizes how these options have been applied by NSIDC, and provides an approximate estimate of the effects of applying or not applying the different options. Currently, NSIDC has only performed comparisons on these processing options for the SSM/I DMSP-F8 and -F11 data. A similar assessment for DMSP-F13 data will be added to this online report upon completion of data comparison.

Introduction

Before converting the DMSP SSM/I antenna temperatures (T_as) to brightness temperatures ($T>_b$s), Wentz (1993) recommends making adjustments to the T_as for two types of systematic errors. The first error appears to result because the feedhorn partially sees the cold-space reflector at the edge of the Earth-viewing portion of the scan. As a result, a systematic roll-off of the T_a values occurs starting near scan position 100, and reaches a maximum value of about 1 Kelvin at the final scan position, 128. Wentz performs an along-scan correction to fix this problem. Figure 1 shows the recommended along-scan T_a correction coefficient as a function of the SSM/I scan position for the F8 and F11 platforms.

The second correction recommended by Wentz is a cross calibration of the various SSM/I platforms. This adjustment is based on intercomparisons between the SSM/I instruments and is performed after the T_a along-scan corrections have been completed. The result is a set of regression coefficients to relate the F10 T_as to those from F8, and the F11 T_as to those from F10. The correction is in the form of the following equations:

Ta10 = (1 - B10)*Ta10 - A10
Ta11 = (1 - B11)*Ta11 - A11

where the B and A coefficients are given in Table 1 for the F10 and F11 platforms.

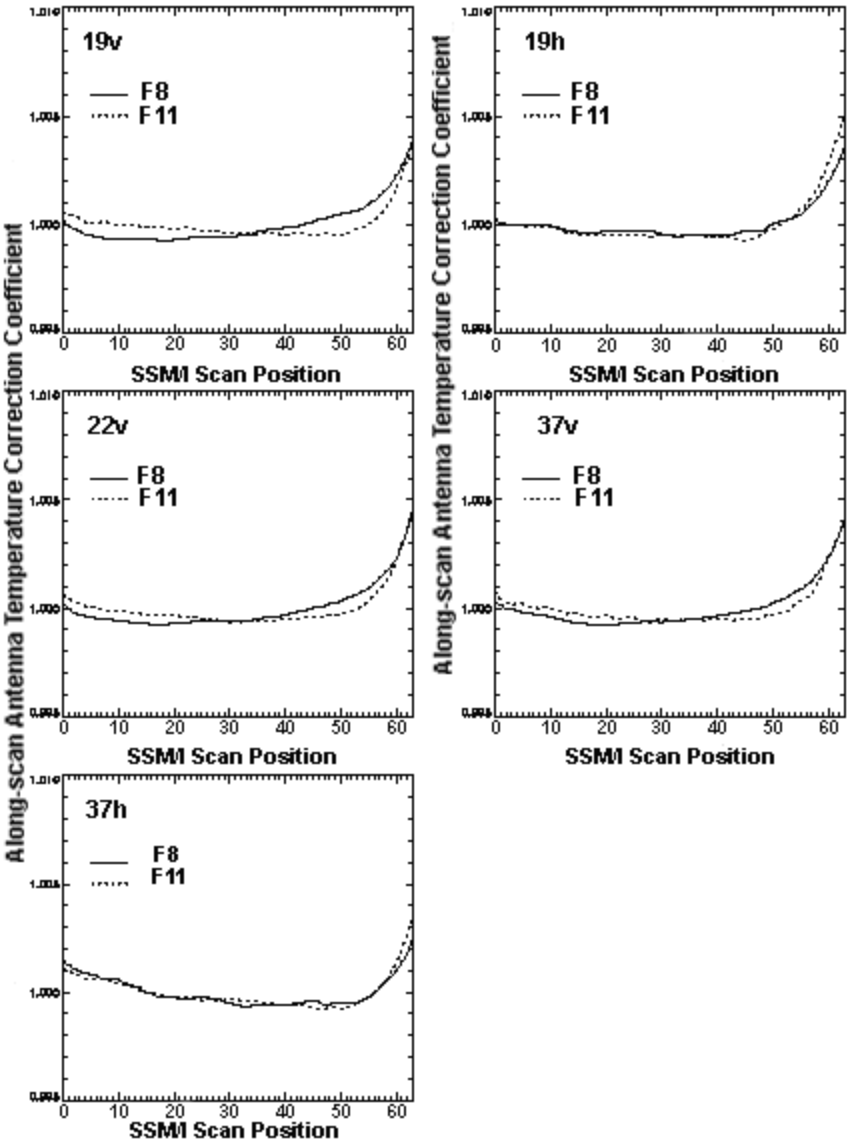

Figure 1. A comparison of the along-scan antenna temperature adjustments between F8 and F11.

Table 1. Cross-sensor intercalibration coefficients for F10 and F11 antenna temperatures (Wentz 1995).

	A10(K)	A11(K)	B10	B11
19V	0.08	0.44	0.00221	0.00221
19H	0.35	-0.16	0.00079	0.00079
22V	-0.33	0.30	0.00161	0.00161

37V	-0.01	-0.01	0.00335	0.00335
37H	0.44	-0.03	0.00165	0.00165

Both of the Wentz adjustments, the along-scan and the intercalibration corrections, are to be applied to the antenna temperatures before they are converted to brightness temperatures. Because it takes Wentz approximately a year after the launch of the SSM/I spacecraft to provide the values for these adjustments, the corrections were not applied to the F11 data set processed at NSIDC. However, the along-scan correction was applied to all of the F8 data. The following paragraphs discuss the impact on the antenna temperatures and resulting brightness temperatures of the F11 along-scan as well as the intercalibration adjustments.

Effects of the Wentz Adjustments on Antenna and Brightness Temperatures

Detailed information on the differences in antenna and brightness temperatures are compared below using the Wentz F11 along-scan and intercalibration adjustments versus not using these adjustments. In this section, the input antenna temperatures are assumed to be constant along the scan, set at either 150, 250 or 350 K. Although this is not the case in reality, it provides an estimate of the maximum error expected along the scan for a given temperature. The impact of the adjustments for real antenna temperatures is discussed shortly.

In Table 2, the impact of the along-scan corrections on the resulting antenna temperatures are shown for the three different antenna temperatures. The expected maximum differences along the scan for a given input antenna temperature are given in the table. The impact of the along-scan adjustment on the antenna temperatures increases with increasing antenna temperature. Thus, for an antenna temperature of 350 K, differences of almost 2 K may be expected, if the along-scan adjustment is not included in the data processing.

Table 2. Minimum and maximum differences in antenna temperatures between using the Wentz F11 along-scan correction versus not using the along-scan correction. The results are presented assuming three different magnitudes for the input antenna temperature.

Channel	**TA=150K**		**TA=250K**		**TA=350K**	
	min	**max**	**min**	**max**	**min**	**max**
19v	-0.0783997	0.587921	-0.130661	0.979858	-0.182922	1.37180
19h	-0.115173	0.771637	-0.191956	1.28609	-0.268768	1.80048
22v	-0.0903778	0.688232	-0.150635	1.14706	-0.210907	1.60587
37v	-0.0990143	0.629425	-0.165024	1.04904	-0.231018	1.46866
37h	-0.113617	0.549164	-0.189362	0.915268	-0.265106	1.28137

Table 3 provides results of the along-scan correction on the corresponding brightness temperatures. In computing the magnitude of the along-scan adjustment, we assumed that the horizontal and vertical antenna temperatures were equal. As for the antenna temperatures, the magnitude of the change in brightness temperature with the along-scan adjustments applied increases with increasing antenna temperature. The impact of the along-scan adjustments were slightly greater for the brightness temperatures than for the antenna temperatures.

Table 3. Minimum and maximum differences in brightness temperatures between using the Wentz F11 along-scan correction versus not using the along-scan correction. The results are presented assuming three different magnitudes for the input antenna temperature.

Channel	**TA=150K**		**TA=250K**		**TA=350K**	
	min	**max**	**min**	**max**	**min**	**max**
19v	-0.0811768	0.606613	-0.135254	1.01105	-0.189362	1.41544
19h	-0.119797	0.801208	-0.199646	1.33539	-0.279541	1.86948
22v	-0.0921783	0.701935	-0.153625	1.16992	-0.215088	1.63788
37v	-0.100876	0.639389	-0.168137	1.06567	-0.235382	1.49191
37h	-0.116287	0.556015	-0.193787	0.926682	-0.271301	1.29736

The impacts of the intercalibration corrections on the F11 antenna temperatures are shown in Table 4. Since the impact of this adjustment is not dependent on the SSM/I scan position, values presented are constant along the scan, assuming a constant antenna temperature of either 150, 250 or 350K. As expected the magnitude of the correction increases with increasing antenna temperatures, but in general, the impact of the intercalibration adjustment is not as large as that of the along-scan adjustment. At an antenna temperature of 350K, differences in excess of 1K occur at 19[V] and 37[V].

Table 4 also shows the maximum impact of the along-scan and intercalibration adjustments recommended by Wentz on the resulting brightness temperatures. Except at 19[H], the combination of both the recommended Wentz adjustments result in maximum differences that are positive (e.g. where the unadjusted brightness temperature is less than the adjusted brightness temperature). Again, we find that as the input antenna temperature increases, the impact of the corrections on the brightness temperatures also increases. At 19[H], differences of almost 2 K are found at Ta = 350 K.

Table 4. Comparison of antenna (left) and brightness temperatures (right) using the Wentz F11 intercalibration correction versus not using the intercalibration correction. The results are presented assuming three different magnitudes for the input antenna temperature.

Antenna Temperatures						Brightness Temperatures	
Channel	**TA=150 K**	**TA=250 K**	**TA=350 K**	**Channel**	**TA=150 K**	**TA=250 K**	**TA=350 K**
19v	-0.77	-0.99	-1.21	**19v**	-0.80	-1.03	-1.26
19h	0.04	-0.04	-0.12	**19h**	0.06	-0.02	-0.09
22v	-0.54	-0.70	-0.86	**22v**	-0.55	-0.72	-0.88
37v	-0.49	-0.83	-1.16	**37v**	-0.50	-0.84	-1.19
37h	-0.21	-0.38	-0.55	**37h**	-0.22	-0.38	-0.55

Table 5. Comparison of brightness temperatures using the Wentz F11 intercalibration and along-scan correction versus not using the intercalibration correction. The results are presented assuming three different magnitudes for the input antenna temperature.

Channel	TA=150K		TA=250K		TA=350K	
	min	**max**	**min**	**max**	**min**	**max**
19v	0.193776	0.881566	0.0183669	1.16467	-0.157042	1.44777
19h	-0.845915	0.0714016	-1.29750	0.231385	-1.74906	0.391369
37v	-0.0990143	0.629425	-0.217508	1.01876	-0.300637	1.43013
37h	-0.113617	0.549164	-0.548258	0.572024	-0.755150	0.813242
22v	-0.149591	0.644537	-0.453316	0.870246	-0.757042	1.09594

Table 6. Maximum negative and positive differences of the along-scan, intercalibration, and both the along-scan and intercalibration adjustments on the resulting brightness temperatures for the Northern and Southern Hemispheres during June 1995.

Channel	Along-Scan		Intercalibration		Both	
	Northern	**Southern**	**Northern**	**Southern**	**Northern**	**Southern**
	min	**max**	**min**	**max**	**min**	**max**

19v	-1.2, 0.3	-1.0, 0.2	0.0, 1.1	0.0, 1.1	-0.1, 1.3	0.0, 1.2
19h	-1.5, 0.2	-1.3, 0.2	-0.1, 0.1	-0.1, 0.1	-1.4, 0.3	-1.3, 0.3
22v	-1.4, 0.2	-1.2, 0.2	0.0, 0.8	0.0, 0.8	-0.6, 1.0	-0.5, 1.0
37v	-1.3, 0.2	-1.1, 0.2	0.0, 1.0	0.0, 0.9	-0.3, 1.2	-0.3, 1.1
37h	-1.1, 0.3	-0.9, 0.2	0.0, 0.5	0.0, 0.4	-0.6, 0.7	-0.6, 0.6

The impact of the Wentz adjustments is slightly greater in the Northern than in the Southern Hemisphere. This is a result of slightly higher antenna temperatures over the Northern Hemisphere during summer. As noticed in the above simple calculations, the along-scan adjustments have a greater overall effect on the brightness temperatures (in terms of greatest magnitude of the differences). However, the effect is most pronounced at the edge of the scan (Figure 2), consequently the adjustment is minimal for most of the image with temperature differences well under 1 K. In contrast, the intercalibration adjustments have a larger overall impact on the entire image (Figure 3). At 19[H], the effect of the intercalibration adjustments is, at most, 0.1 K. However, for the vertically polarized channels, differences of around 1 K are found for most of the image. Figure 4 shows the impact on the brightness temperatures of both the along-scan and intercalibration adjustments.

Figure 2. Effect of the along-scan adjustments on the brightness temperatures in the Northern Hemisphere on 1 June 1995.

Figure 3. Effect of the intercalibration adjustments on the brightness temperatures in the Northern Hemisphere on 1 June 1995.

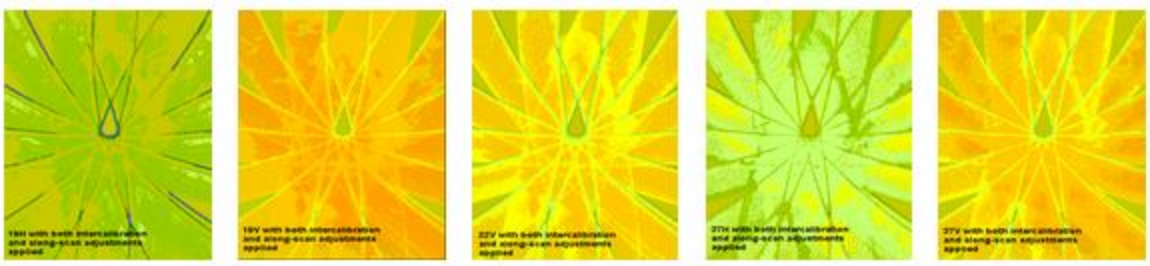

Figure 4. Effect of the along-scan and intercalibration adjustments on the brightness temperatures in the Northern Hemisphere on 1 June 1995.

Effects of the Wentz Adjustments on Sea Ice Concentrations

The next step was to determine the overall effect of the Wentz adjustments on sea ice concentrations derived from the adjusted or unadjusted brightness temperatures. Even though the adjustments had a substantial impact on the brightness temperatures, the effects may be minimal on the resulting sea ice fractions. To test the results of the above adjustments, total ice fractions for both hemispheres were generated using the NASA Team and Bootstrap sea ice algorithms.

NASA Team

In Figure 5, differences in total ice fractions between using no adjustments and (a) intercalibration, (b) along-scan and (c) both the Wentz adjustments are shown for the Northern Hemisphere on 1 June 1995. Figure 6 shows the results for the Southern Hemisphere. From the figures we find that the along-scan adjustments have a negligible impact on the resulting ice fractions, with differences on the order of 0-0.2 percent for both hemispheres. However, individual pixels exist that have differences as large as 40 percent (Northern Hemisphere) and 30 percent (Southern Hemisphere). These spurious large differences in total ice result from pixels in either the adjusted or unadjusted data that are filtered out as weather, whereas the same pixel in the other data set is not. Thus, in some instances, the brightness temperature differences are large enough to influence the weather filter criteria.

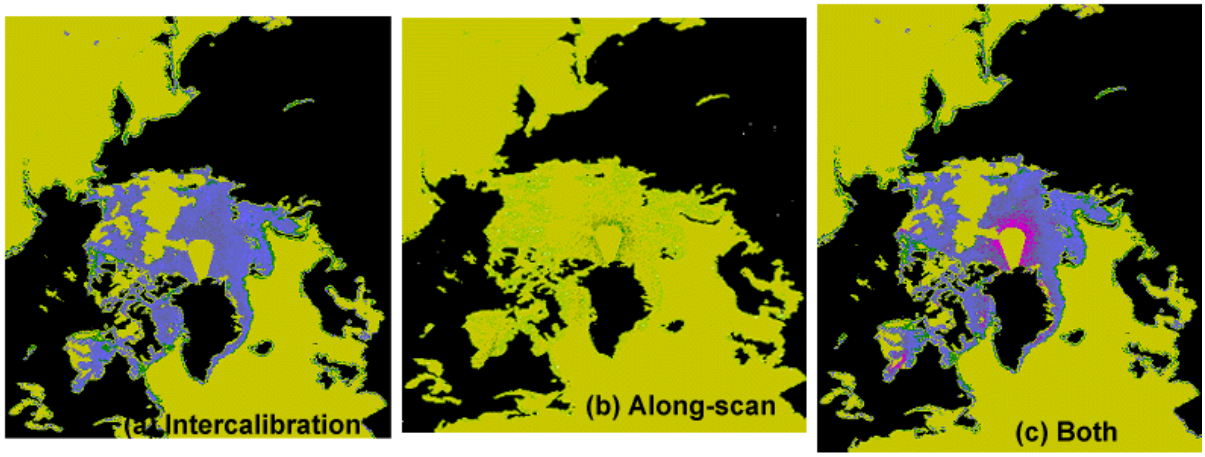

Figure 5. Differences in Northern Hemisphere total ice fractions between using no adjustments and (a) intercalibration, (b) along-scan and (c) both adjustments.

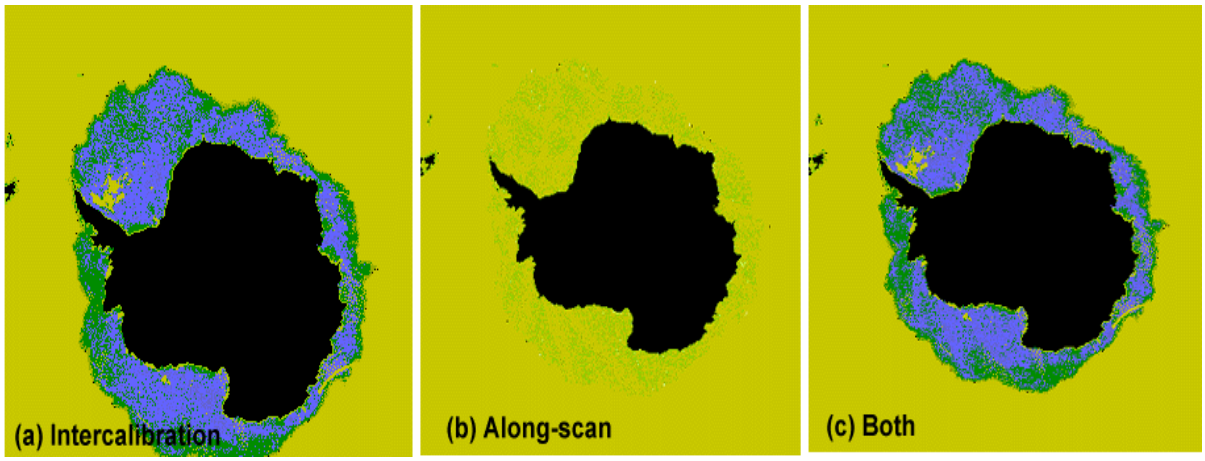

Figure 6. Differences in Southern Hemisphere total ice fractions in the Southern Hemisphere between using no adjustments and (a) intercalibration, (b) along-scan and (c) both adjustments.

Larger differences in total ice fraction are observed when the intercalibration corrrections are applied to the brightness temperatures. In the interior of the ice pack, differences on the order of 1.2 percent (Northern Hemisphere) and one percent (Southern Hemisphere) are found, where the adjusted data predicts greater ice fractions than the unadjusted data. At the ice edge and along the coastlines, the differences decrease to about 0.6 percent. However, it is interesting that there is a large area in the interior of the ice pack, northwest of the pole, where the differences in ice fractions are approximately zero. A similar pattern of near zero ice fractions is observed using the Comiso algorithm (see Figure 7a). Larger differences are found for a few isolated pixels, as large as 70 percent in the Northern Hemisphere, 30 percent in the Southern Hemisphere. As noted before, the large differences result from the weather filter labeling the pixel as open water for one data set, but not for the other. Effects of intercalibrations on ice concentrations are discussed in more detail in Stroeve et al. (1998).

Applying both the along-scan and intercalibration brightness temperature adjustments, differences in total ice concentrations increase slightly, most notably near the pole in the Northern Hemisphere (1.6 percent). It is only near the pole in the Northern Hemisphere where the along-scan adjustments have a noticeable effect on the ice concentrations, and this is reflected in the ice fractions using both the Wentz adjustments. Overall, the combination of both corrections results in greater ice fractions for both hemispheres than the uncorrected ice fractions.

Bootstrap

Figures 7 and 8 show the differences in total ice fractions between using no adjustments and (a) intercalibration, (b) along-scan and (c) both the Wentz adjustments for the Northern and Southern Hemispheres, respectively, using the Comiso sea ice algorithm. The ice fractions are computed for 1 June 1995. As observed with the NASA Team ice fractions, the intercalibration adjustments have a greater impact than the along-scan adjustments on the resulting ice fractions. Using only the along-scan corrections, differences of a similar magnitude occur in the Northern Hemisphere, with a few exceptions. In the interior of the ice pack, isolated pixels with differences on the order of 15 percent are found. Near the pole, positive differences of around 0.5 percent occur, and west and southeast of the Greenland ice sheet, there are pixels with differences up to 10 percent.

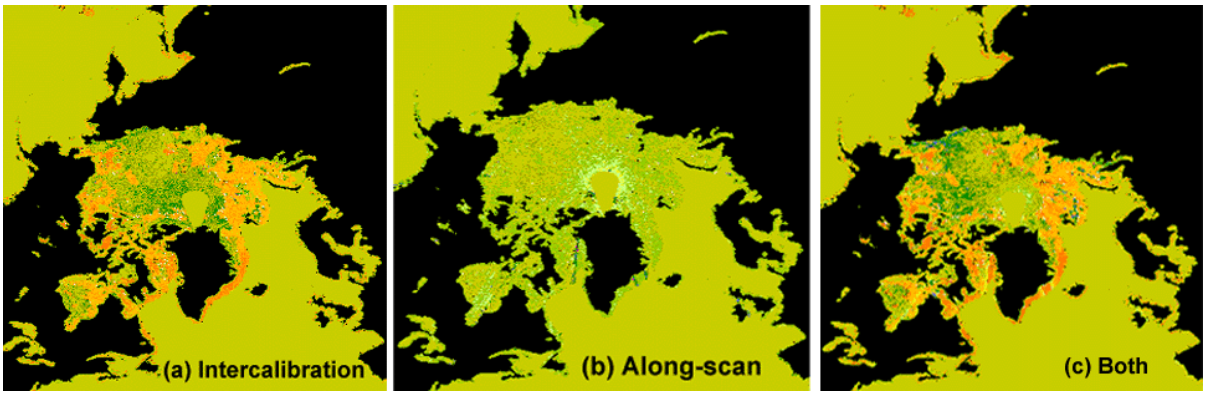

Figure 7. Effects of intercalibrations on ice concentrations in the Northern Hemisphere.

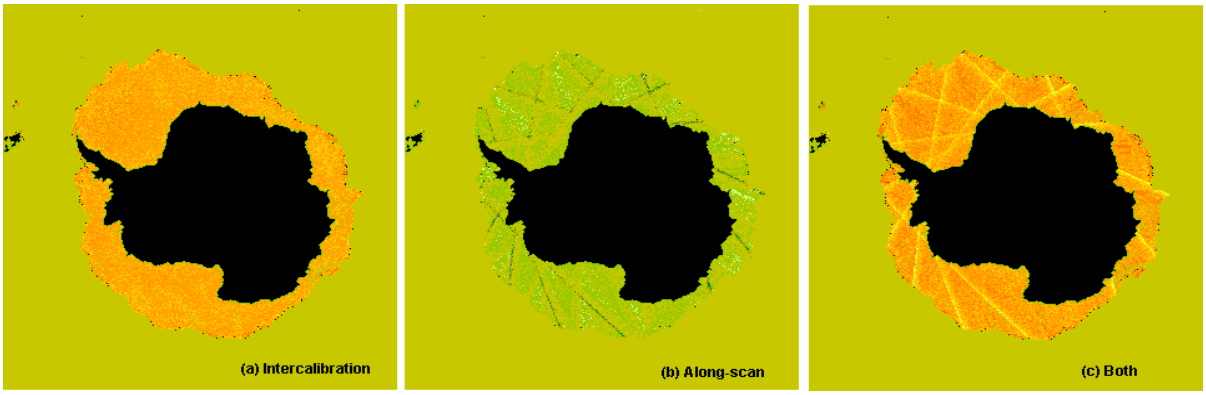

Figure 8. Effects of intercalibrations on ice concentrations in the Southern Hemisphere.

In the Southern Hemisphere, most of the consolidated ice has differences on the order of zero to 0.3 percent. However, at the edge of the scan the differences increase to about 0.5 percent (adjusted total ice fractions are greater than the unadjusted ice fractions). There are also individual pixels along the ice margin at the edge of the scan line that have differences of almost 10 percent. It is interesting to note that using the Bootstrap sea ice algorithm, the locations of the individual scan lines remain evident in the total ice fractions, especially in the Southern Hemisphere. This occurs because the Bootstrap algorithm uses individual brightness temperatures, whereas the NASA Team algorithm uses ratios of the brightness temperatures in computing the ice fractions. In the Northern Hemisphere the maximum difference is 70 percent, and the maximum difference is 45 percent in the Southern Hemisphere. Again, slight differences in the brightness temperatures cause some pixels to be filtered by the weather filter and others not.

In the Southern Hemisphere, the intercalibration adjustments result in differences that are very homogenous throughout the ice pack. Differences on the order of one percent are found. Isolated pixels, found predominately along the ice margin, exist with differences well in excess of 10 percent. In the Northern Hemisphere, the unadjusted total ice fractions are about 1.3 percent greater than the intercalibrated ice fractions in the marginal ice zones. Near the pole, the differences tend to reduce to around 0.5 percent (adjusted > unadjusted), and decrease even further to around 0.1 percent for the rest of the consolidated ice. There remain however, isolated pixels in the interior of the ice and along the ice edge with differences in excess of 10 percent. The maximum difference is 65 percent.

Finally, Figures 7 [c] and 8 [c] show the differences in ice fractions using both of the Wentz adjustments for the Northern and Southern Hemisphere, respectively. The differences in total ice concentrations are similar to those observed using the intercalibration adjustments, except in areas where the along-scan adjustments have noticeable effects. In general, the along-scan and intercalibration corrections tend to cancel each other in the Bootstrap-derived ice fractions. Thus, a reduction is seen in the total ice fraction differences when compared to those using just the intercalibration corrections in locations where the along-scan have their greatest impact. For example, in the Southern Hemisphere, the differences in ice concentrations shrink from one percent to around 0.5 percent at the edge of the scan. In contrast, when using the NASA Team algorithm, an increase in ice fraction differences was found in the Northern Hemisphere where the along-scan adjustments had their greatest effect (e.g. near the pole). Furthermore, using the Bootstrap sea ice algorithm, the Wentz adjustments result in smaller ice fractions for both hemispheres than the unadjusted data set, whereas the reverse was found using the NASA Team algorithm.

References

Stroeve, J., J. Maslanik and X. Li. 1998. An intercomparison of DMSP F11- and F13-derived sea ice products. *Remote Sens. Env.* 64:132-52.

Wentz, F. J. 1995. Final report, production of SSM/I data sets. Remote Sensing Systems, Inc., Santa Rosa, CA. RSS Technical Report 090192.

Wentz, F. J. 1993. User's manual: SSM/I antenna temperature tapes. rev. 2. Remote Sensing Systems, Inc. Santa Rosa, CA. RSS, Technical Report 120193.